

LOW MISSING MASS, SINGLE- AND DOUBLE DIFFRACTION DISSOCIATION AT THE LHC

L. Jenkovszky^{1,2,a}, A. Saliı̄^{1,b}, J. Turóci^{3,c} and D. Himics^{3,d}

¹ Bogolyubov Institute for Theoretical Physics, National Academy of Sciences of Ukraine
UA-03680 Kiev, Ukraine

² Wigner Research Centre for Physics, Hungarian Academy of Sciences 1525 Budapest,
POB 49, Hungary

³ Uzhorod State University

^a jenk@bitp.kiev.ua, ^b saliı̄.andriy@gmail.com, ^c turoczi.jolika@citromail.hu, ^d himicsdia@hotmail.com

ABSTRACT. Low missing mass, single- and double diffraction dissociation is calculated for the LHC energies from a dual-Regge model. The model reproduces the rich resonance structure at low mass region, and approximate behavior for high mass-region.

1. Introduction

Measurements of single (SD) double (DD) and central (CD) diffraction dissociation (Dif.) are among the priorities of the Large Hadron Collider (LHC) at CERN.

In the past, intensive studies of high-energy diffraction dissociation were performed at the Fermilab, on fixed deuteron target, and at the ISR, see [1] for an overview and relevant references. One can see the rich resonance structure there, typical of low missing masses, often ignored by extrapolating this region by a simple $1/M^2$ dependence. When extrapolating (in energy), one should however bear in mind that, in the ISR region, secondary Reggeon contributions are still important (their relative contribution depends on momentum transfer considered), amounting to nearly 50% in the forward direction. At the LHC, however, their contribution in the nearly forward direction is negligible, i.e. less than the relevant error bars in the measured total cross section [3].

This new situation makes diffraction at the LHC unique in the sense that for the first time Regge-factorization is directly applicable.

2. Pre-LHC measurements: ISR, Fermilab and Tevatron (CDF)

Previous to the LHC, single diffraction dissociation was intensively studied at the ISR the Fermilab (fixed deuteron target) and at the Tevatron in the range of $14 < \sqrt{s} < 1800 \text{ GeV}$, $|t| < 2 \text{ GeV}^2$, and missing masses ranging from the threshold up to $\xi < 0.15$. The main results of these measurements and of their theoretical interpretation can be summarized as follows, for details see, e.g. [1, 2]:

1. Energy dependence. At the ISR and Fermilab energies the integrated SD cross section rises with s according to the standard prescription of the Regge-pole theory, however it slows down beyond. This effect was expected due to the familiar problem related to the violation of unitarity, namely that at high energies, implying the triple Pomeron limit, the D cross section overshoots the total cross section, $\sigma_{SD} > \sigma_T(s)$. Various means were suggested [5] to remedy this deficiency, including decoupling (vanishing) of the triple Pomeron vertex. Goulianos renormalizes the standard Pomeron flux to meet the data, see [2]. Such a “renormalization” produces a break near $\sqrt{s} \approx 20 \text{ GeV}$ slowing down the rise of $\sigma_{SD}(s)$ in accord with the CDF data from the Tevatron.

We instead will cure this problem by using rudiments of a dipole Pomeron (DP), compatible with unitarity without any renormalization factor, that produces a sharp (non-analytic) change in the behavior of $\sigma_{SD}(s)$: a dipole Pomeron (double Pomeron pole) is compatible with unitarity, in particular in the sense that both the SD cross section rises proportionally with the total cross section. The DP produces logarithmically growing cross sections at unit Pomeron intercept, however to meet the observed

rise of the ratio σ_{el}/σ_{tot} , the Pomeron intercept is allowed to be slightly beyond unity, namely, $\alpha_{IP}(t)=1.04$. In other words, the rise of the cross sections is driven both by the dipole (by a logarithmic factor) and a tiny (half of Donnachie-Landshoff's [8] supercritical intercept).

2. *t-dependence* of σ_{SD} and the slope $B(s; t; M^2)$ was calculated in the range $0.01 < t < 2GeV^2$. Although nothing dramatic was found (the diffraction cone essentially is exponential in t , the shape of the diffraction cone is DD may contain important detail to be unveiled by future measurements: a dip similar to that in elastic scattering is likely to appear (near $t \sim 1GeV^2$). Another important issue in the behavior of the cone of Dif. is a possible turn-down towards small- t due to the kinematical factor, denoted below by $F(t, M^2)$, connecting the pP structure function with the total cross section (see Sec. IV). This tiny effect is located in the kinematical region where Coulomb interaction is sizable. However, as noticed in Ref. [4], in DD processes, the Coulomb interaction, at small squared momentum transfers, is suppressed compared to that in elastic diffractive pp scattering, allowing for a better determination of the strongly interacting part of the amplitude (in pp ; at small t this is possible only indirectly, by means of the Bethe-Heitler interference formula).

3. *M²-dependence*. The data compilation for SD processes from different experiments (ISR, Fermilab, Tevatron e.g. see Ref. [1]) shows that the small- M^2 region, is full of resonances. In most of the papers on the subject this resonance structure is ignored and it is replaced by a smooth function $\sim M^{-2}$ allegedly approximating the resonances. Moreover, this simple power-like behavior is extended to the largest available missing masses. In sec. IV we question this point on the following reasons: a) the low- M^2 resonances introduce strong irregularities in the behavior of the resulting cross sections; b) the large- M^2 behavior of the amplitude (cross sections) is another delicate point. Essentially, it is determined by the proton-Pomeron (pP) total cross section, proportional to the pP structure function, discussed in details in Sec. IV. By duality, the averaged contribution from resonances sums up to produce high missing-mass Regge behavior $(M^{-2})^n$, where n is related to the intercept of the exchanged Reggeon (essentially, that of the f trajectory). Furthermore, according to the ideas of two-component duality, see e.g. [7], the cross sections of any process, including that of $pP \rightarrow X$, is a sum of a non-diffractive component, in which resonances sum up in high-energy (here: mass) Regge exchanges and the smooth background (below the resonances) is dual to a Pomeron exchange. The dual properties of Diff. can be quantified also by finite mass sum rules, see [1]. In short: the high-mass behavior of the $pP \rightarrow X$ cross section is a sum of a decreasing term going like $\sim M^{-2}$ and a "Pomeron exchange" increasing slowly with mass. All this has little affect on the low-mass behavior at the LHC, however normalization implies calculation of cross sections integrated over all diffraction region up to $\xi < 0.05$.

3. Factorization relation

So, with the advent of the LHC, diffraction, elastic and inelastic, entered a new area, where it can be seen uncontaminated by non-diffractive events. In terms of the Regge-pole theory this means, that the scattering amplitude is completely determined by a Pomeron exchange, and in a simple-pole approximation, Regge factorization holds and it is of practical use! Note that the Pomeron is not necessarily a simple pole: pQCD suggests that the Pomeron is made of an infinite number of poles (useless in practice), and the unitarity condition requires corrections to the simple pole, whose calculation is far from unique. Instead a simple Pomeron pole approximation [8] proved to be efficient in describing a variety of diffractive phenomena.

The DL elastic scattering amplitude is simply:

$$A(s, t) = \xi(t)\beta(t)(s/s_0)^{\alpha_{IP}(t)-1} + A_R(s, t), \quad (1)$$

where $\xi(t) = e^{i\pi/2}$ is the signature factor, and $\alpha_{IP}(t) = 1.04 + 0.25t$ is the Pomeron trajectory. The residue is chosen to be a simple exponential, $\beta(t) = e^{b_p t}$

with $b_p = 8.4GeV^{-1}$ [3]. "Minus one" in the power of (1) anticipates of norm $\sigma_{tot}(s) = \text{Im}A(s, t=0)$ the scale

parameter s_0 isn't fixed by the Regge-pole theory: it can be fitted do the data or fixed to a "plausible" value of a hadronic mass, or to the inverse "string tension" (inverse of the Pomeron slope), $s_0 = 1/\alpha'$ according to DL. The second term in Eq. (1), correspond to sub-leading Reggeons, has the same functional form as the first one (Pomeron), just the values of the parameters differ. We ignore this term for reason mentioned above.

Factorization of the Regge residue $\beta(t)$ and the "propagator" $(s/s_0)^{\alpha_{IP}(t)-1}$ is a basic property of the theory. As mentioned, at the LHC for the first time, we have the opportunity to test directly Regge-factorization, since the scattering amplitude is dominated by a simple Pomeron-pole exchange, identical in elastic and inelastic scattering. Simple factorization relations between elastic, single and double are known from the literature [1].

$$\frac{d^3\sigma_{DD}}{dt dM_1^2 dM_2^2} = \frac{d^2\sigma_{SD}}{dt dM_1^2} \frac{d^2\sigma_{SD}}{dt dM_2^2} \bigg/ \frac{d\sigma_{el}}{dt} \quad (2)$$

4. Model for single and double diffraction dissociation

The construction of our model relies on the following premises:

1. *Regge factorization*. This is feasible since, as stressed repeatedly, at the LHC energies and for $t < 1GeV^2$, typical of diffraction, the contribution from secondary Reggeons is negligible, and, for a single Pomeron term, factorization is exact;

2. Due to factorization, the relevant expressions for the cross sections (elastic, SD, DD) are simple, as written

below, (3-5). Such relations are known from the literature, see e.g. [1] and references therein;

3. The inelastic pPX vertex receives special care. Following Refs. [9,10] we consider this vertex as a deeply inelastic process, similar to the $\gamma p \rightarrow X$ vertex in lepton-hadrons DIS e.g. at HERA or JLab. The virtual photon of DIS here is replaced by the (virtual) Pomeron with an obvious change of Q^2 typical of DIS to $-t$ in the present $pP \rightarrow X$ sub-processes the total c.m. energy here being M . There is one important difference between the two, namely the quantum numbers of the Pomeron and the photon (positive and negative C parities, respectively). However, this is not essentially since the dynamics is the same and the produced states in the pP system will be those of the relevant nucleon trajectory with the right quantum numbers (see below). Contrary to Jaroszewicz and Landshoff [10], who use the Regge asymptotic (in the missing mass) form of the Pp structure function and, consequently the triple Pomeron limit, leaving outside the low- M resonance region with and use a "Reggeized Breit-Wigner" formula for the structure function elaborated in ref.[9] (see also earlier citations therein). By duality, the relevant sum of the two parts (low- and high missing mass) should be equivalent. This interesting feature of Dif. was studied in the 70-ies (see [1] and references therein), and it merits to be revived.

4. *The background* is always a delicate issue. In the reactions (SD, DD) under consideration there are two sources for the background. The first is that related to the t channel exchange and can be accounted for by rescaling the parameter s_0 in the denominator of the Pomeron propagator. In any case, at high energies, i.e. those of the LHC, this background is included automatically in t -channel Pomeron exchange. The second type of background comes from the sub processes $pP \rightarrow X$. The Pp total cross section at high energies (here: missing masses) has two components: a decreasing one dual to direct-channel resonances and going as $M^{2\alpha(0)}$, where $\alpha(0)$ is the intercept of the effective (non-leading) Regge trajectory exchanged in the cross-channel of the sub process, and a background below the resonances, whose dual is a slowly rising term. There is some freedom in choosing the background and they are important in fixing the normalization, compatible with earlier measurements.

In this section we consider only single (SD) and double (DD) diffraction dissociation of the proton at LHC energies. Central diffractive production will be treated elsewhere. We follow the dual-Regge approach of Ref. [9], but simplify the expressions for Pp inelastic form factors (transition amplitudes) by replacing them with high-energy Pomeron-proton total cross sections, dominated by Pomeron exchange. The resulting cross sections are:

$$\frac{d^2\sigma_{el}}{dt} = A_{el} F_p^4(t/s_0)^{2(\alpha(t)-1)}, \quad (3)$$

$$\frac{d^2\sigma_{SD}}{dt dM_x^2} = F_p^2(t) F(x_B, t) \frac{\sigma_T^{pp}(t, M_x^2)}{2m_p} (s/M_x^2)^{2(\alpha(t)-1)} \ln(s, M_x^2), \quad (4)$$

$$\frac{d^3\sigma_{DD}}{dt dM_1^2 dM_2^2} = C_n F^2(x_B, t) \frac{\sigma_T^{pp}(t, M_1^2)}{2m_p} \frac{\sigma_T^{pp}(t, M_2^2)}{2m_p} \times (s/(M_1 + M_2)^2)^{2(\alpha(t)-1)} \ln(s/(M_1 + M_2)^2), \quad (5)$$

$$\sigma_T^{pp}(M_x^2, t) = \text{Im} A(M_x^2, t) = \frac{A_{N^*}}{\sum_n n - \alpha_{N^*}(M_x^2)} + Bg(t, M^2) = \quad (6)$$

$$= A_{norm} \sum_{n=0,1,\dots} \frac{[f(t)]^{2(n+1)} \text{Im} \alpha(M_x^2)}{(2n+0.5 - \text{Re} \alpha(M_x^2))^2} + Bg(t, M^2),$$

where:

$$\alpha(t) = \alpha(0) + \alpha' t, \quad f(t) = e^{b_{in} t},$$

$$F_p(t) = \frac{1}{1 - \frac{t}{0.71}},$$

$$F(x_B, t) = \frac{-t(1-x_B)}{4\pi\alpha_s(1+4m^2x_B^2/(-t))}, \quad (7)$$

$$Bg(t, M^2) = B_{norm} e^{b_{bg} t} (M^2 - M_{p+\pi}^2)^\epsilon. \quad (8)$$

5. Results

Table 1: Parameters set

$\sigma_{SD} (mb)$	10.2	16.4
$\sigma_{SD}(M < 3.5 GeV) (mb)$	4.8	5.4
$\sigma_{SD}(M > 3.5 GeV) (mb)$	5.4	11.0
$\sigma_R^{SD} es (mb)$	3.6	3.3
$\sigma_B^{SD} g (mb)$	6.6	13.1
$b_{in} (GeV^{-2})$	0.2	0.2
$b_{in}^{bg} (GeV^{-2})$	3	3
$\alpha' (GeV^{-2})$	0.25	0.25
$\alpha(0)$	1.04	1.04
ϵ	1.03	1.06
A_{norm}	27.0	25.0
B_{norm}	5.0	8.0

As the input, elastic cross section and the slope of the cone for elastic cross section for pp scattering from TOTEM were also used:

$$\sigma_{el}(7TeV) = 24.8 \pm 0.2 \pm 1.2 mb$$

$$B_{el}(7TeV) = 20.1 \pm 0.2 \pm 0.3 GeV^{-2}$$

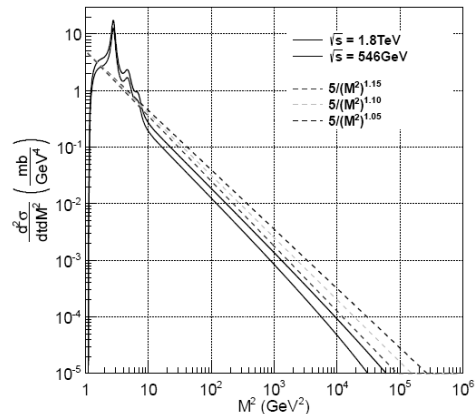


Figure 1: Double differential cross sections, $t = -0.05$. Comparison to of calculated cross section reference line (see. Fig.3,a). $\sigma_{SD} \approx 10mb$.

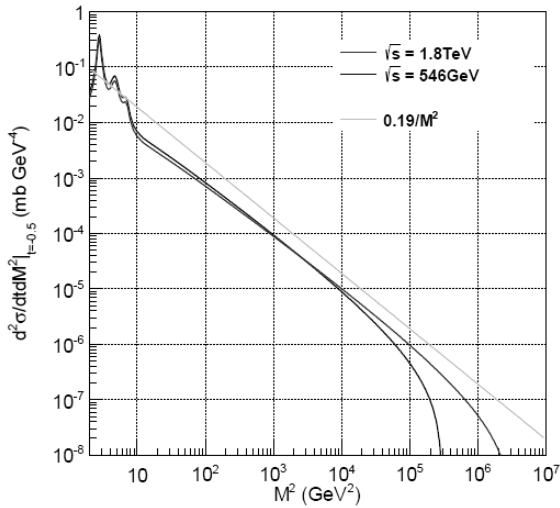


Figure 2: Double differential cross sections, $t = -0.05$. Comparison of calculated cross section to the reference line (see. Fig.3, b). Normalization: $\sigma_{SD} \approx 10mb$.

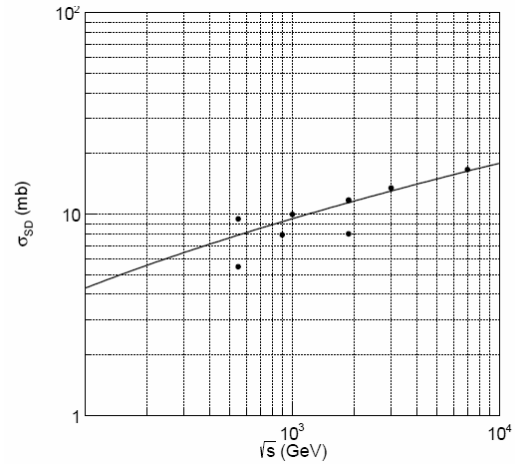
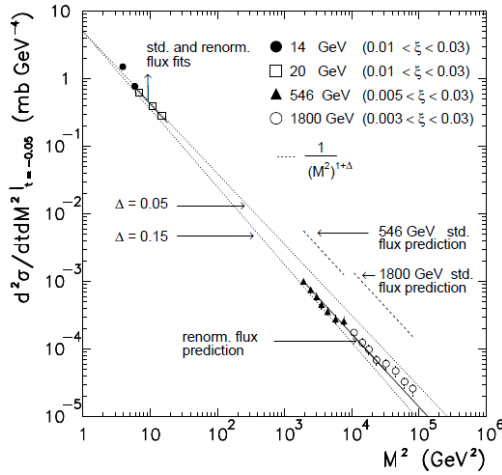
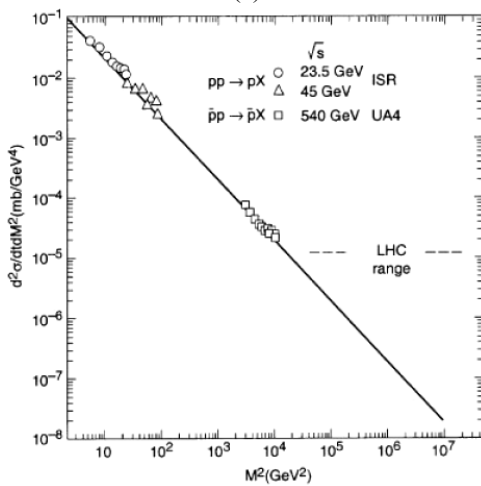


Figure 4: Single diffraction cross section vs. \sqrt{s} . Normalization: $\sigma_{SD} \approx 10mb$.



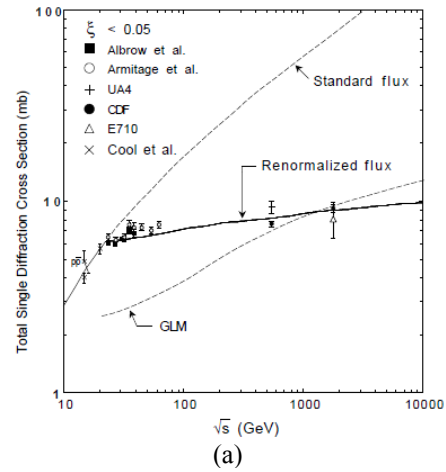
(a)



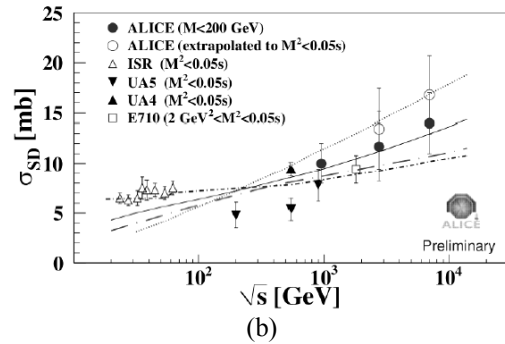
(b)

Figure 3: Reference points for $\frac{d^2 \sigma_{SD}}{dt dM^2}$.

- (a) For $t = -0.05$, from [7];
- (b) For $t = -0.5$, form [8].



(a)



(b)

Figure 5: Single defraction cross section vs. \sqrt{s} .

- (a) Goulianos [7];
- (b) With the new preliminary points form ALICE [9].

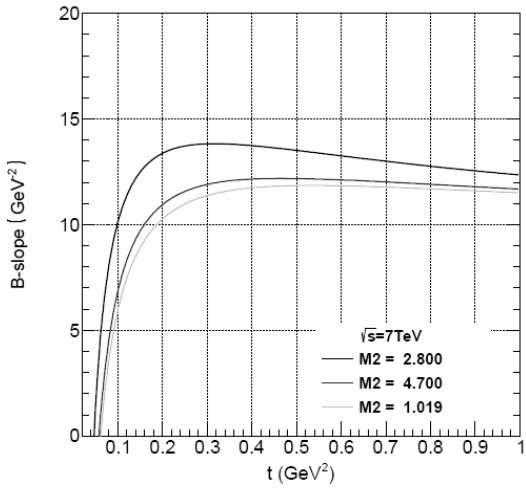


Figure 6: B-Slopes for differential SD cross section as a function of t for appropriate M^2 values. with normalization $\sigma_{SD} \approx 10mb$.

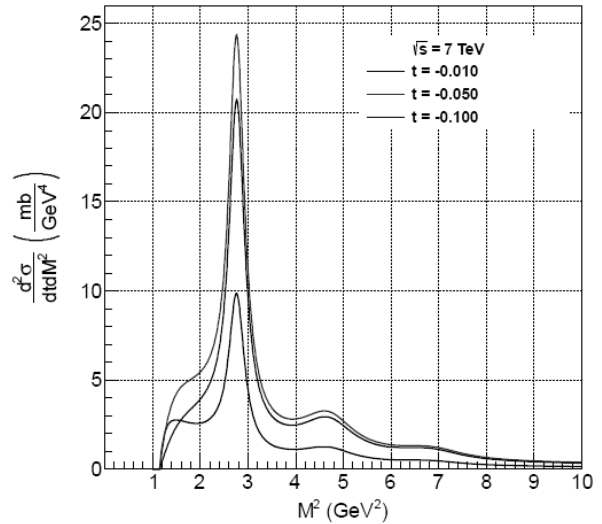


Figure 9: Double differential SD cross sections as a function of M^2 for different t values. normalization $\sigma_{SD} \approx 10mb$.

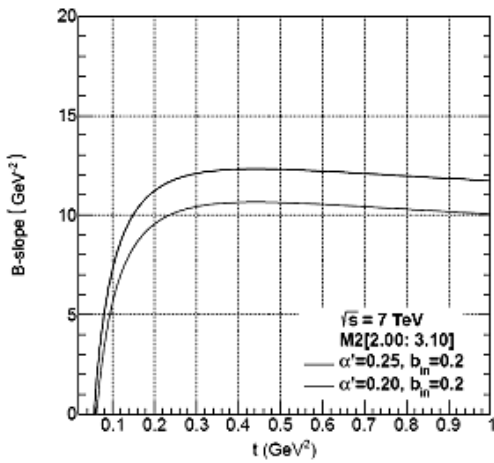


Figure 7: B-Slopes for differential SD cross section integrated in the region of the first resonance $M \in [2.0: 3.1 GeV^2]$. Normalization $\sigma_{SD} \approx 16$.

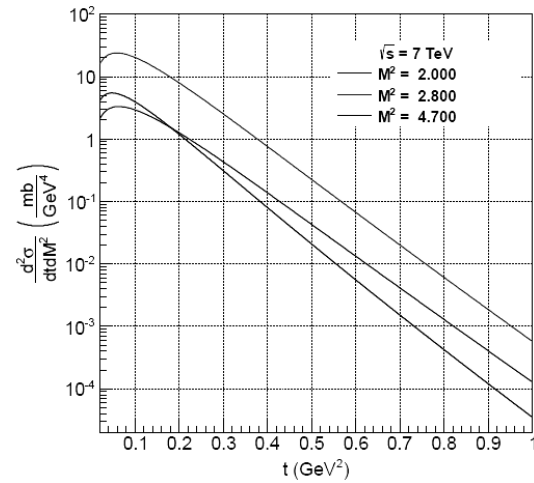


Figure 10: Double differential SD cross sections as a function of t for different M^2 values. Normalization $\sigma_{SD} \approx 10mb$.

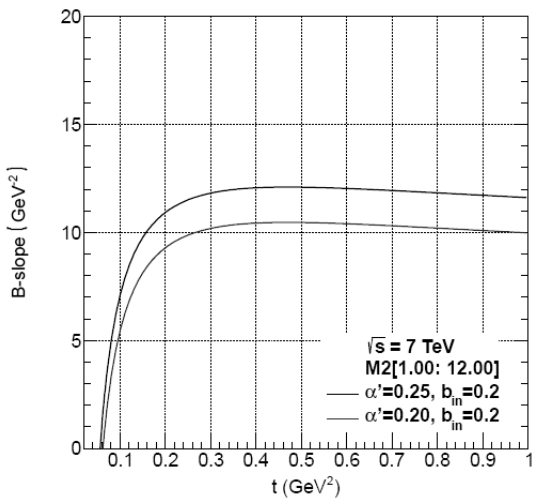


Figure 8: B-Slopes for differential SD cross section integrated in the region of the resonances $\sigma_{SD} \approx 10mb$, normalization $\sigma_{SD} \approx 10mb$.

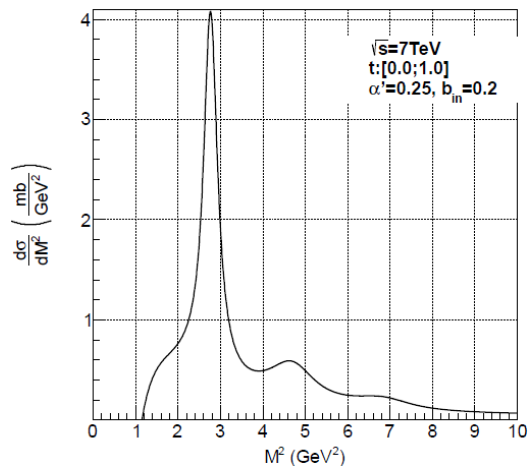


Figure 11: Single differential SD cross sections as a function of M^2 integrated over the region $t \in [0.0:1.0]$, normalization $\sigma_{SD} \approx 10mb$.

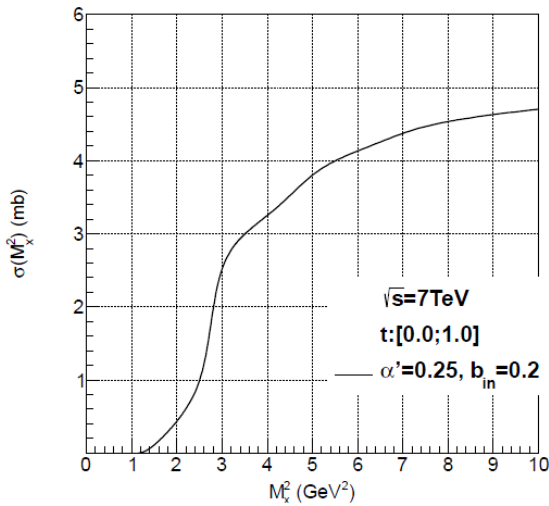


Figure 12: SD cross section as a function of upper M_x^2

$$\text{bound. } \sigma_{SD}(M_x^2) = \int_1^{M_x^2} \frac{d\sigma_{SD}}{dM^2} dM^2, \quad \frac{d\sigma_{SD}}{dM^2} = \int_{-1}^0 \frac{d\sigma_{SD}}{dt} dt$$

Normalization $\sigma_{SD} \approx 16$.

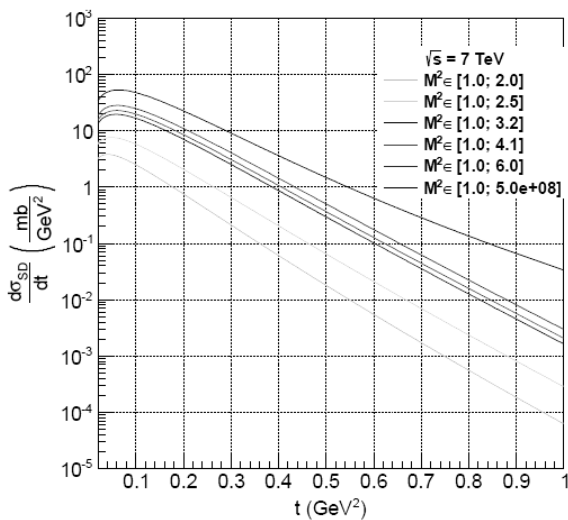


Figure 13: Single differential SD cross sections integrated in different M^2 regions as a function of t , normalization $\sigma_{SD} \approx 10mb$.

Acknowledgements. L. J. is grateful to the organizers of this Gamov conference, especially to Professors M.Ryabov and A.Zhuk for their invitation and for the pleasant and creative atmosphere during the conference.

References

1. Goulianos K.: 1983, *Phys. Rep.*, **101**, 169.
2. Goulianos K.: *In Proc. 13th International Conf. on Elastic and Diffractive Scattering (Blois Workshop) Moving Forward into the LHC Era*, hep-ph/1002.3527, p. 6; 121.
3. Jenkovszky L., Lengyel A., Lontkovskiy D.: 2011, *Int. J. Mod. Phys. A*, **26**, **27**, 4755-4771.
4. Goulianos K., Jenkovszky L.L., Struminsky B.V.: 1991, *Yad. Fizika*, **54**, 573.
5. Roy D.P., Roberts R.G.: 1974, *Nucl. Phys. B*, **77**, 246.
6. Jenkovszky L., Martynov E., Paccanoni F.: 1996, in *Proc. of the Crimean Conference on Diffraction*.
7. Fiore R., Jenkovszky L., Magas V., Melis S., Prokudin A.: 2009, *Phys.Rev., D* **80**, 116001, arXiv:0911.2094.
8. Donnachie S., Dosch G., Landshoff P., Nachtmann O.: 2002, *Pomeron physics and QCD*, Cambridge University Press.
9. Jenkovszky L., Kuprash O., Lamsä J., Magas V., Orava R.: 2011, *Phys.Rev.*, **D83**, 056014, arXiv:hep/ph/1011.0664.
10. Jaroszewicz G.A., Landshoff P.V.: 1974, *Phys. Rev.*, **10**, 170.
11. Antchev G. et.al.: 2011, CERN-PH-EP-2011-158, hep-exp/1110.1395.
12. Fiore R., Jenkovszky L., Magas V., Paccanoni F., Papa A.: EPJ A10 (2001); 217-221, hep-ph/0011035 (2000).
13. Poghosyan M.G.: 2011, arXiv:1109.4510 [hep-ex].
14. Goulianos K.: 2001, *Nucl.Phys.Proc.Suppl.*, **99A**, 9, arXiv:hep-ex/0011060v1.
15. Bozzo A. et.al.: 1984, *Phys. Letters*, **B136**, 217.
16. Matthiae G.: 2000, *Brazilian Journal of Physics* **30**, 30, sciELO, 244.